Calorimetric determination of inhibition of ice crystal growth by antifreeze protein in hydroxyethyl starch solutions

Thomas N. Hansen and John F. Carpenter
CryoLife, Incorporated, Marietta, Georgia 30067 USA

ABSTRACT Differential scanning calorimetry and cryomicroscopy were used to investigate the effects of type I antifreeze protein (AFP) from winter flounder on 58% solutions of hydroxyethyl starch. The glass, devitrification, and melt transitions noted during rewarming were unaffected by 100 μg/ml AFP. Isothermal annealing experiments were undertaken to detect the effects of AFP-induced inhibition of ice crystal growth using calorimetry. A premelt endothermic peak was detected during warming after the annealing procedure. Increasing the duration or the temperature of the annealing for the temperature range from −28 and −18°C resulted in a gradual increase in the enthalpy of the premelt endotherm. This transition was unaffected by 100 μg/ml AFP. Annealing between −18 and −10°C resulted in a gradual decrease in the premelt peak enthalpy. This process was inhibited by 100 μg/ml AFP. Cryomicroscopic examination of the samples revealed that AFP inhibited ice recrystallization during isothermal annealing at −10°C. Annealing at lower temperatures resulted in minimal ice recrystallization and no visible effect of AFP. Thus, for 100 μg/ml AFP to have a detectable influence on thermal events in the calorimeter, conditions must be used that result in significant ice growth without AFP and visible inhibition of this process by AFP.

INTRODUCTION

Ice crystals can greatly damage cryopreserved biological material (1, 2). Fahy and co-workers (3) suggested that problems associated with ice formation could be avoided by the use of vitrification. At ultralow temperatures, the water matrix in the vitrified (glassy) state has the same "random" structure as in the liquid state, but with the loss of translational motion (4, 5). Red blood cells, for example, have been cryopreserved by vitrification using ultrarapid cooling in the presence of the extracellular cryoprotectant hydroxyethyl starch (HES) (6–8). In such samples, however, the glassy state is metastable. During rewarming damage due to ice can occur (3, 5), with the spontaneous formation of new ice nuclei (devitrification) and the growth of ice crystals. The ice crystal growth may represent either an increase in ice mass (crystallization) or in a rearrangement of crystals without an increase in mass (recrystallization). All of these kinetic phenomena can be avoided by using rapid warming rate (5), but warming rates become increasingly limited as the sample volume increases.

Ice growth can also be reduced by the addition of antifreeze protein (AFP) to the solutions. AFP has been shown to inhibit recrystallization of ice formed by ultrarapid cooling of solutions during isothermal annealing between −8 and −4°C (9–11). Such inhibition can be beneficial to cryopreserved cells. For example, we have found that 5–100 μg/ml type I AFP (from winter flounder) enhanced survival of red cells that were cryopreserved in 23% (wt/wt) solutions of HES and rewarmed at suboptimal rates (12). Cryomicroscopic examination revealed that this protective effect correlated with the visible inhibition of ice recrystallization by AFP (12).

Address correspondence to Dr. Thomas N. Hansen at CryoLife, Inc., 2211 New Market Parkway, Suite 142, Marietta, GA 30067.

Dr. John F. Carpenter's current address is: University of Colorado Health Sciences Center, Denver, CO 80262.

Previous research with much higher concentrations of AFP (1–200 mg/ml) in 55% (wt/wt) glycerol demonstrated that the addition of AFP shifted the glass transition to warmer temperatures and the devitrification to lower temperatures (13). To determine whether similar physical effects might contribute to the increased survival induced by the lower concentrations of AFP used in our red cell cryopreservation model, we used differential scanning calorimetry to examine the influence of 100 μg/ml AFP on the glass, devitrification, and melt transitions in HES solutions. Our initial experiments indicated that 100 μg/ml AFP did not have any detectable effect on these thermal transitions during a single warming scan. However, after isothermal annealing a premelt endotherm was present during the subsequent scan. The endotherm probably represents the transition in the non-ice portion of the HES solution (14–16). The enthalpy of the peak decreased with increasing annealing time or temperature > −16°C, but remained higher in the solution with AFP compared with the solution without AFP. Cryomicroscopy revealed that recrystallization of visible ice crystals was inhibited by AFP under identical annealing conditions.

MATERIALS AND METHODS

Materials

Purified (>99% homogeneity) antifreeze protein was a gift from Dr. J. E. Villafranca of Agouron Pharmaceuticals, Inc. (La Jolla, CA). The recombinant protein was produced by expression of a synthetic gene in *Escherichia coli*. The protein has a molecular weight of 3,300, is comprised of 37 amino acids, and has an amino acid sequence identical to that of the natural, type I antifreeze protein from winter flounder (*Pseudopleuronectes americanus*), which is designated as HPLC-6 (cf., 17).

HES (average 450,000 M_r and seven ethyl substitutions per 10 anhydroglucose residues) was purchased from Kendall McGaw Laboratories (Santa Ana, CA). Solutions of 30 and 58% (wt/wt) were prepared by dissolving the HES in deionized water containing from 0 to 100

0006-3495/93/06/1843/08 $2.00

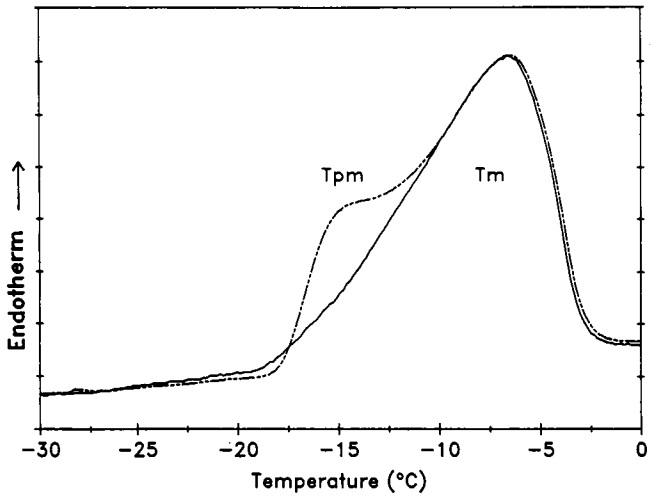

FIGURE 1 Thermograms of 58 wt% HES with and without isothermal annealing at −15°C, illustrating how the premelt endotherm enthalpy was calculated. The same sample was scanned twice, once from −170 to +5°C without annealing (*solid line*) and once with a 30-min annealing at −15°C before recooling and rewarming (*dashed line*). The premelt endotherm (*Tpm*) overlapped the melt endotherm (*Tm*) after the annealing. To calculate the enthalpy of *Tpm*, the total area of the endotherm (*Tpm* + *Tm*) was subtracted from the area of the melt endotherm obtained without any hold: (*Tpm* + *Tm*) − *Tm* = *Tpm*. These calculations assume that the melt peak does not change with various hold conditions. The melt peak enthalpy after holds at −28°C (where the two peaks do not overlap) did not change after annealing.

μg/ml AFP or bovine serum albumin. We limited ourselves to this range of AFP concentrations because we previously found that this range enhanced survival of red cells cryopreserved in HES, whereas higher concentrations fostered damage (12). The HES was used as obtained from the manufacture and thus contained NaCl. Salt is necessary for formation of a stable α-helix conformation in type I AFP (18).

Calorimetry

Calorimetric analysis of the solutions was performed in a liquid nitrogen–cooled calorimeter (model DSC-7; Perkin-Elmer Cetus Instruments, Norwalk, CT). Samples of HES solution between 1 and 5 mg were placed in 20-μl aluminum pans for volatile samples. The samples were covered with immersion oil to prevent sample dehydration during isothermal annealing experiments. In initial experiments the sample was cooled as rapidly as possible to −170°C by using the "Go to Load" function. The cooling rate was determined empirically to be ≥200°C/min to −80°C but was increasingly slower between −80 and −170°C. Data were collected during a 10°C/min scan from −170 to +5°C. The glass transition, devitrification, and melting temperatures and enthalpies were determined. For isothermal annealing experiments, the sample was rapidly cooled to −170°C and warmed (20°C/min) to a temperature between −28 and −8°C. The sample was held at the given temperature for a duration of 0–120 min. After the hold, the sample was recooled to −50°C and data were collected during a 10°C/min scan from −50 to +5°C. All conditions were tested with a minimum of three individual samples, and values are reported as mean ± 1 SD. Paired Student's *t* test was used for statistical analysis of the data.

The enthalpy value of the premelt endotherm obtained during the warming scan after annealing was determined by measuring peak area. When the premelt and melt peaks overlapped in the scan after annealing, the total peak area was noted. To determine how much of the total enthalpy was due to the premelt event, the melt peak recorded during the initial scan, without annealing, was subtracted from the total enthalpy obtained after annealing (Fig 1). Triplicate runs of the same sample revealed that the premelt peak enthalpy values were reproducible to ±1.7% at −28°C and to ±2.5% at −10°C.

Cryomicroscopy

The solutions were also monitored visually using a liquid nitrogen–cooled microscope stage (Interface Techniques Co., Cambridge, MA), with computer temperature control. The sample (~1 mg) was placed on the stage and cooled at 200°C/min to −135°C. It was then warmed to −28, −15, or −10°C and held at that temperature for 30 min. The sample was monitored for ice recrystallization using a video camera (Sony CCD-IRIS) connected to a video printer (Sony color video printer UP-5000). Micrographs were taken at 0, 10, and 30 min.

RESULTS

Initial calorimetry experiments were with 30% (wt/wt) HES solutions, a similar concentration used for cryopreservation of red blood cells (12). Thermograms revealed no glass transition or devitrification during rewarming, after cooling at the maximum rate in the calorimeter. This was probably because samples could not be cooled rapidly enough in the calorimeter to become vitreous. Körber et al. (19) also reported no devitrification in solutions at concentrations < 55 wt%, when cooled at 320°C/min. Thus, higher HES concentrations that could form a glass upon cooling at ~200°C/min were used (19). A typical thermogram obtained from 58 wt% HES is presented in Fig 2. The glass transition (*Tg*) onset appeared at −106°C, with the midpoint inflection at −94°C, and the end of the transition at −72°C. Devitrification (*Td*) occurred over a range from −72 to −29°C, whereas a small endotherm preceding the melt occurred over a range from −26.5 to −18.6°C. The temperature values obtained for the transitions were similar to those previously reported (19). The addition of 100 μg/ml

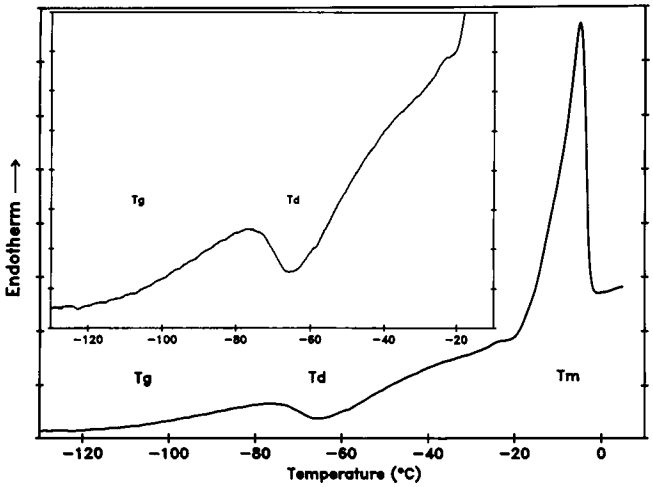

FIGURE 2 Thermogram of 58 wt% HES. The sample was cooled as rapidly as possible to −170°C and then warmed at 10°C/min. The glass transition (*Tg*), devitrification (*Td*), and melt (*Tm*) are labeled. (*Inset*) −130 to −10°C portion of the thermogram is presented to better reveal the transitions.

AFP did not influence any of these transitions. The thermograms of samples containing AFP were essentially indistinguishable from those for samples without AFP.

Because AFP did not influence the phase transitions in HES solutions during a single cooling and rewarming regime, we conducted isothermal annealing experiments to maximize the opportunity to detect AFP-induced inhibition of ice growth calorimetrically. Annealing times of ≤4 h between −100 and −72°C had no effect on the glass or devitrification temperatures or enthalpies in the presence or absence of AFP. Annealing the HES solution in the absence of AFP at −28°C, the end of the devitrification event, or at higher temperatures resulted in the loss of the glass and devitrification transitions and in the appearance of a premelt endotherm after subsequent cooling and scanning during rewarming (Fig 3). The peak gradually moved towards the melt as the annealing temperature increased and, after annealing at −15°C, appeared as a shoulder on the melt. The premelt endotherm had almost disappeared after 30 min at −10°C (Fig 3). The onset temperature of the premelt peak was directly correlated with the annealing temperature. The relationship was linear, with the onset temperature shifting from −23.5 to −18°C (best-fit curve equation: $y = 0.44x - 11.2$, for $-28 \leq x \leq -16$°C, $r = 0.99$). At annealing temperatures > −16°C the peak onset no longer shifted but was superimposed on the melt peak.

The first annealing experiment with AFP compared the effect of 100 μg/ml of the protein on the samples held for 30 min at −28 and −10°C. AFP did not alter the

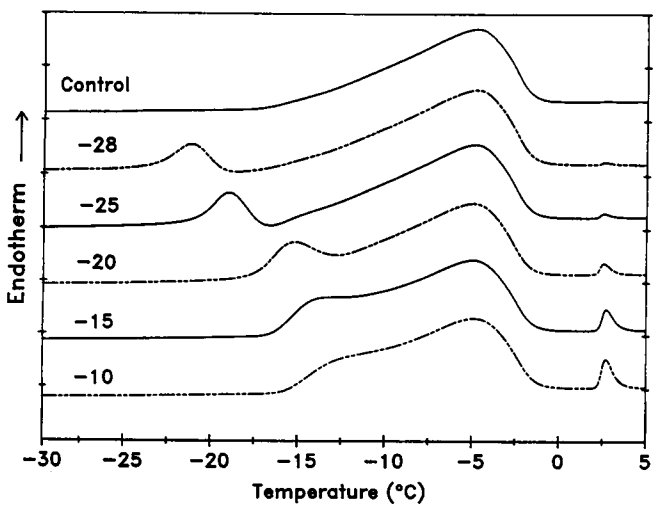

FIGURE 3 Thermograms of 58 wt% HES solutions after a 30-min isothermal annealing at various temperatures. After annealing, the sample was recooled and data were collected during a warming scan. The premelt endothermic peak was readily apparent after the annealing regimes, either as a distinct endotherm or as a shoulder on the melt. The various annealing temperatures are labeled above each curve (control = no annealing). The postmelt peak (at 2.5°C) was an artifact of sample evaporation and recondensation (19). Covering the sample with immersion oil greatly minimized and, in some cases eliminated, the postmelt peak.

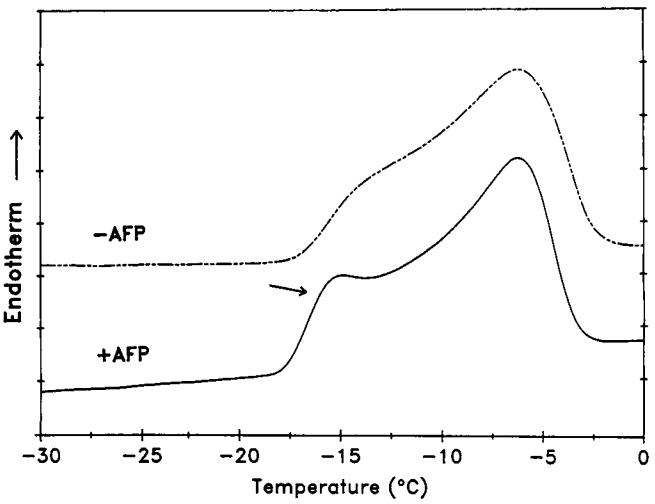

FIGURE 4 Thermograms of 58 wt% HES solutions annealed at −10°C for 30 min before analysis. The solutions contained 0 (*dashed line*) or 100 μg/ml AFP (*solid line*). The premelt peak endotherm obtained during a warming scan after annealing appeared as a slight shoulder in the sample without AFP but was still pronounced in the solution with AFP (*arrow*).

enthalpy or position of the premelt endotherm after annealing at −28°C. However, a sample annealed at −10°C in the presence of 100 μg/ml AFP had a much larger enthalpy than a control sample without the protein (Fig 4). Similar effects were noted at AFP concentrations down to 10 μg/ml (data not shown).

If the appearance of the premelt endotherm is due to ice growth and recrystallization and the effect of AFP is due to inhibition of these processes during the annealing period, then these events should be altered by the duration of the annealing. To examine the kinetic nature of these phenomena, samples of HES with and without AFP were annealed at −28 and −10°C for 0 to 120 min. The samples were then recooled and data were collected during rewarming. As the annealing time at −28°C increased from 0 to 30 min, the onset temperature of the premelt peak shifted from −28 to −24°C. No further shift was observed with increased annealing times up to 120 min. The premelt peak enthalpy gradually increased with duration of annealing up to 30 min and did not change with longer annealing (Fig 5). The enthalpy of the premelt endotherms for samples with AFP (Fig 5) were not statistically different from those for control samples without the protein ($P > 0.4$). When solutions were annealed at −10°C, the onset temperature of the premelt peak remained at −18°C for all annealing times, whether AFP was present. AFP also did not influence the enthalpy of the peak after 0–5 min annealing (Fig 6). However, after 15 min or longer, the premelt peak enthalpy for the solution without AFP decreased, whereas the enthalpy for the solution with AFP remained constant (Fig 6). No differences were noted between samples containing 100 μg/ml bovine serum albumin and

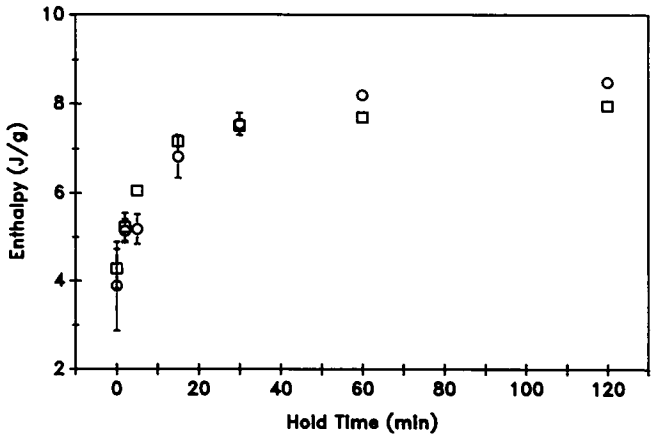

FIGURE 5 Effect of various annealing times at −28°C on the premelt peak enthalpy. The enthalpy values were measured directly, since the premelt and melt peaks did not overlap (see Fig 3). No difference in the measured enthalpy was noted for samples held 30 min or longer. Also, no statistical difference ($P > 0.4$) was noted between samples with (□) or without (○) 100 μg/ml AFP.

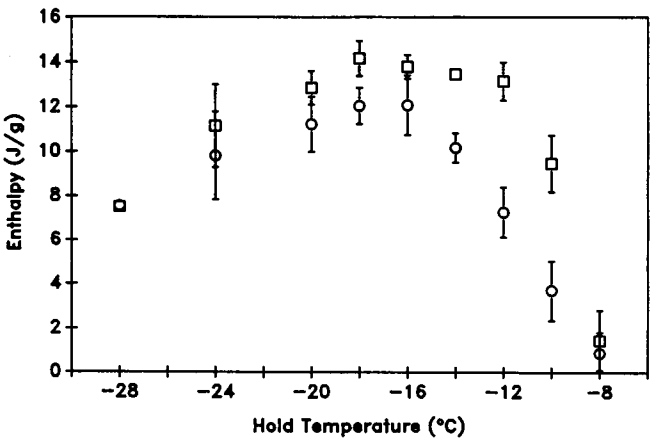

FIGURE 7 Effect of various annealing temperatures on the premelt enthalpy. Samples either with 100 μg/ml AFP or without any protein were recooled and data collected during a warming scan after a 30-min annealing at various temperatures. Symbols: (○) 58 wt% HES; (□) 58 wt% HES + 100 μg/ml AFP.

the control samples (Fig 6), demonstrating that the effect is specific to AFP.

Because the kinetic studies indicated that the enthalpy of the premelt endotherm had reached a steady state after 30 min of annealing at −28 or −10°C, this time period was chosen for experiments comparing intermediate annealing temperatures (Fig 7). Statistical differences in the enthalpy of the premelt peak between the two types of samples began to emerge at −16°C ($P < 0.05$) were greatest at −12 and −10°C ($P \leq 0.025$) but were no longer noted at −8°C ($P > 0.4$) deep into the sample melt.

Taken together the results presented above suggest that the appearance of the premelt endotherm noted after isothermal annealing is associated with ice growth during the annealing. The peak might also be due to a eutectic melt of the NaCl in the HES solution (20). However, certain aspects of our data argue against this interpretation. First, the peak shifted to warmer temperatures with higher annealing temperatures. A eutectic melt temperature would be invariant, whereas kinetic phenomena have been shown to shift with the application of differing thermal and holding regimes (15, 21). Second, HES, which was dialyzed extensively against deionized water to remove all salts, was analyzed as above. The same premelt endotherm was noted after annealing at −28°C (data not shown).

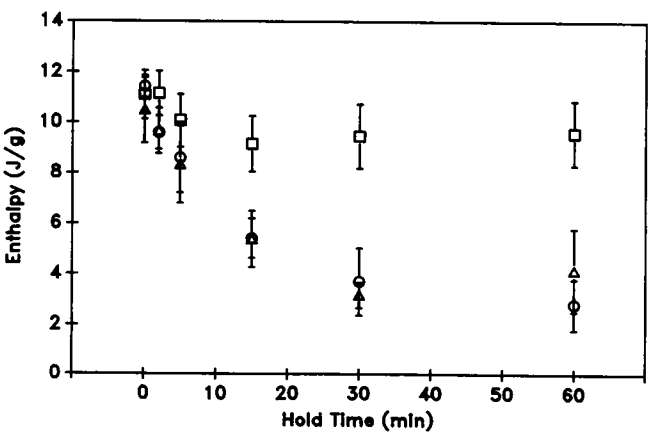

FIGURE 6 Effect of various annealing times at −10°C on the premelt peak enthalpy. The enthalpy values were determined as in Fig 1, because the premelt and melt peaks overlapped. (○) 58 wt% HES; (□) HES + 100 μg/ml AFP; (△) HES + 100 μg/ml bovine serum albumin.

To ascertain more directly under which annealing conditions ice recrystallization was occurring and the effects of AFP on this process, the HES samples were examined using cryomicroscopy. The solutions were subjected to the same cooling and annealing regimes as in the calorimeter. Upon cooling to −130°C, the solutions appeared clear and remained optically transparent during warming until ~ −20°C. At this point the field became gradually darker, indicating ice crystal growth (22). The field became brighter during annealing at −10°C, as ice recrystallization progressed and allowed for better resolution of individual crystals. Immediately upon reaching −10°C there were visible ice crystals of essentially the same size, both in samples with and without AFP (Fig 8). After 10 min about the same degree of ice crystal growth was noted. However, the inhibition of recrystallization by AFP was clearly apparent after 30 min at −10°C. These results correlate reasonably well with the calorimetric finding that ≥15 min at −10°C was needed before a noticeable influence of AFP on the premelt endotherm could be detected. Measurement of the larger ice crystals after 30 min revealed that in the solution without AFP the crystals were on average ~49.6

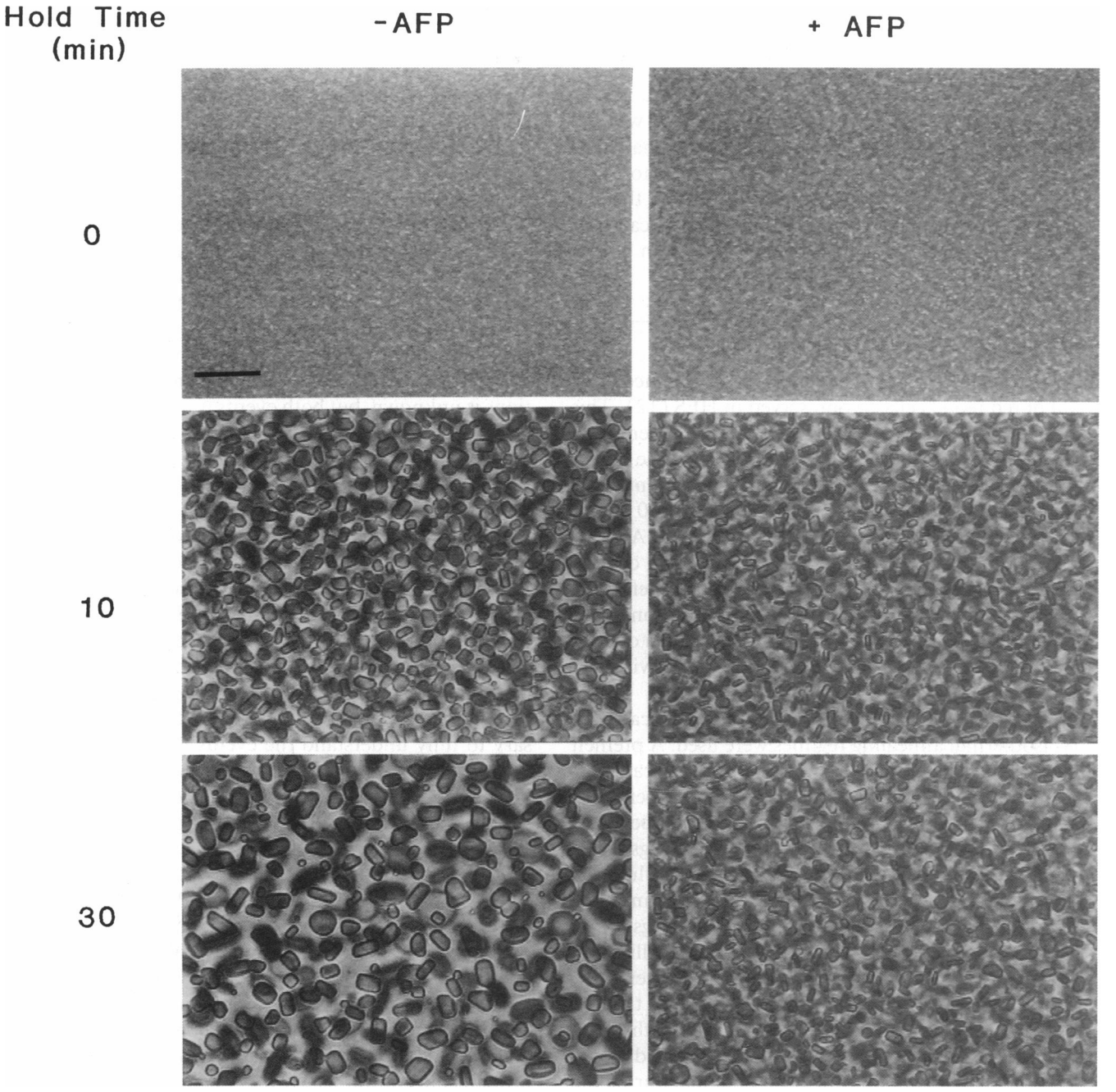

FIGURE 8 Cryomicrographs of 58 wt% HES solution with or without 100 μg/ml AFP. The samples were treated to the same cooling and -10°C annealing as in the calorimeter. Photographs were taken after 0, 10, and 30 min. Bar, 10 μm.

μm^2, whereas in the solution with AFP the crystals were $\sim 14.0\ \mu m^2$ (Fig 8).

Samples were also examined after 30 min annealing at -15 and -28°C, where calorimetric data revealed little or no influence of AFP on the premelt endotherm. After 30 min at -15°C, there were no discernable differences in the appearance of samples with and without AFP. Both appeared similar to the -10°C time zero micrographs, with much opacity due to numerous crystals that were too fine to resolve individually. AFP also did not alter the appearance of samples held at -28°C. Both remained optically clear, with almost no discernable opacity (data not shown).

Finally, to gain some insight into the events occurring during the final postannealing recooling and rewarming (when calorimetric data were collected), samples were annealed at -10°C for 30 min. They were then recooled to -50°C and rewarmed at 10°C/min, as in the calorimeter experiments. As the samples approached the melting temperature during rewarming, there was a clearing

of the hazy gray, non-ice crystal region in the background. In addition, the beginning of the melt of the smaller ice crystals could be detected. This was followed by the melt of the larger ice crystals. The sequence of events during the melt appeared similar with or without AFP. However, samples containing AFP had smaller ice crystals after annealing and appeared to have more of a hazy gray background (Fig 8). It is possible that the premelt endotherm during the final warming in the calorimetry experiments represents a phase transition in the hazy gray, non-ice crystal region.

DISCUSSION

Previous experiments indicated that AFP enhanced survival of red blood cells cryopreserved in HES (12). This effect was correlated with the microscopic observation that AFP inhibited ice recrystallization during the warming of the samples (12). The results of the current study indicate that, in a concentration range of 10–100 μg/ml AFP, this may be the only significant effect of AFP on the physical transitions in HES solution during cooling and warming. We were unable to detect any effect of AFP on the glass, devitrification or melt transitions in 58 wt% HES solutions during a single warming run or after annealing at temperatures near the glass or devitrification transitions.

In an attempt to detect ice recrystallization by calorimetry, isothermal annealing regimes were used. A premelt endothermic peak resulted during a warming scan after annealing (Figs 3 and 4). At annealing temperatures above −16°C, the enthalpy of the premelt peak remained higher in solutions containing AFP (Figs 6 and 7). Furthermore, the premelt endotherm was influenced by the duration and the temperature of annealing, emphasizing the kinetic nature of the event (Figs 3–7). Also, cryomicroscopy revealed that ice recrystallization occurred during the annealing and that AFP attenuated this process (Fig 8). These observations indicate that the premelt endotherm is associated with ice growth or recrystallization arising during the annealing period. However, the premelt endothermic peak obtained during the final warming scan is not an actual ice growth or recrystallization event. Rather, it is a transition in the system formed as the result of ice growth and recrystallization that occurred during the annealing.

One possible interpretation of the premelt endotherm that resulted after annealing is that the peak represents a phase transition in the HES portion of the solution. This would be consistent with the observed clearing of the hazy gray background during warming after annealing. The nature of the transition is unknown, but several hypotheses include relaxation of the ice–solution interface (23), devitrification (14), and glass transition with an associated endothermic overshoot (15, 16). The endothermic overshoot has been reported in other cryoprotective systems (15, 24) and may represent heat absorbed to compensate for the loss of free energy in glasses undergoing relaxation at temperatures below or at the glass transition (25).

Mathematical modeling and experimental data indicate that when an aqueous solution is rapidly cooled to form a glass and then rewarmed, the solute will increase in concentration as the water forms more ice (5, 26). Although these observations were reported for systems undergoing continuous warming, the slowest warming rates suggest that similar phenomena occur during isothermal annealing. We observed two different events after annealing, depending upon the temperature of annealing: between −28 and −18°C the enthalpy value for the premelt peak increased, whereas between −18 and −8°C, the value decreased. The reason for these observations is unknown, but both events must be explained as a result of ice growth occurring during the isothermal annealing (27). Between −28 and −18°C, ice growth would result in a more concentrated HES solution. As such, a shift in the glass transition and endothermic overshoot to higher temperatures would be expected (19, 21). Also, a greater endothermic overshoot would result as more of the glassy HES solution relaxed (15, 24, 28). However, between −18 and −8°C, as ice growth progressed further, a decrease in enthalpy could occur as a result of less water contributing to the signal of the glassy HES system. These suggestions are purely speculative at this point. Further characterization will be necessary to fully understand the events that occur near the glass, recrystallization, and melt points (19).

The common element in the development and disappearance of the premelt peak is the growth of ice during isothermal annealing. The data thus suggest that in the presence of AFP the solution did not approach equilibrium during isothermal annealing between −16 and −10°C. Ice growth must have been inhibited and thus, the premelt peak enthalpy remained high. Recrystallization of ice would not be expected to result in a change in the solution concentration, because it is a redistribution of ice crystal sizes, and not a change in ice mass (27). Ice growth inhibition by AFP has been well documented at protein concentrations ≥ 1 mg/ml, but not at lower concentrations (e.g., reference 29). However, Knight et al. (30) have reported "some slight growth retardation of ice" with 30 μg/ml winter flounder AFP. Also, the water absorptive capacity of HES is very large: 0.522 g of water absorbed/g of powdered HES (19). If we assume that no AFP is present in the water associated with HES, then the calculated concentration of AFP used in this study would be 192 μg/ml. These observations help support the suggestion that AFP inhibited ice growth in the HES solution at −10°C.

The winter flounder AFP was not able to influence the premelt peak in the calorimeter below −16°C (Fig 7). Also, cryomicroscopic observations revealed no effect of AFP on ice recrystallization after 30 min of annealing ≤ −15°C. The lack of effect may be due to kinetic limita-

tions in our system (2, 31). It is possible that greatly extending the hold times may result in a detectable effect by AFP.

Recrystallization in nonmetallic substances, as Burgers (32) explained, is restricted to grain growth (boundary migration), which occurs through the movement of the boundary layers between two lattice regions. The result is a decrease in the free energy stored in the layers. In an attempt to understand the mechanism by which AFP inhibits recrystallization, Knight and coworkers (10, 11) suggested that impurities would decrease the driving force of recrystallization by reducing the total boundary area by the amount of area the impurities occupy. Also, impurities would create a physical barrier around which water molecules would have to diffuse, further slowing down ice recrystallization (32). However, AFP is much more effective at recrystallization attenuation than other protein molecules (10). This may be due to its unique ice adsorption capabilities, which suggest a lattice match with ice is necessary (33–35). If AFP requires a specific lattice match for ice recrystallization attenuation, then the boundary layers in the frozen solution may have to migrate until they reach a protein molecule in the correct orientation before migration inhibition can occur (11). It is less likely that the AFP molecules could migrate, because they are trapped in a viscous matrix. As a result, AFP would not be able to completely prevent recrystallization, and some ice growth would be noted even in the presence of AFP (Fig 8). In fact, the cryomicroscopic data revealed that recrystallization inhibition by AFP was observed only when ice crystals had grown beyond 14 μm^2 in the solution without AFP.

In conclusion, except for ice recrystallization and possibly some ice growth inhibition near the melt, the addition of AFP concentrations relevant to enhancing cryoprotection (i.e., 10–100 $\mu g/ml$) does not seem to influence any of the physical transitions in the cryoprotectant HES. However, inhibition of ice recrystallization alone during warming can be beneficial to cryopreserved systems (1, 12). Such inhibition does not need to be absolute to enhance cell survival. Simply attenuating microscopically visible ice crystal growth appears to be sufficient.

We thank Drs. V. L. Bronshteyn, A. P. MacKenzie, and P. L. Steponkus for many useful discussions and inputs.

This project was supported through grant number N00014-91-C-0044 from the Office of Naval Research.

Received for publication 5 November 1992 and in final form 19 January 1993.

REFERENCES

1. Pegg, D. E. 1987. Ice crystals in tissues and organs. *In* The Biophysics of Organ Preservation. D. E. Pegg and A. M. Karow, editors. Plenum Publishing Corp., New York. 117–136.
2. Martino, M. N., and N. E. Zaritzky. 1989. Ice recrystallization in a model system and in frozen muscle tissue. *Cryobiology.* 26:138–148.
3. Fahy, G. M., D. R. MacFarlane, C. A. Angell, and H. T. Meryman. 1984. Vitrification as an approach to cryopreservation. *Cryobiology.* 21:407–426.
4. Franks, F. 1985. Biophysics and Biochemistry at Low Temperatures. Cambridge University Press, Cambridge, England. 210 pp.
5. MacFarlane, D. R. 1986. Devitrification in glass-forming aqueous solutions. *Cryobiology.* 23:230–244.
6. Knorpp, C. T., W. R. Merchant, P. W. Gikas, H. H. Spencer, and N. W. Thompson. 1967. Hydroxyethyl starch: extracellular cryophylatic agent for erythrocytes. *Science (Wash. DC).* 157:1312–1313.
7. Lionetti, F. J., and S. M. Hunt. 1975. Cryopreservation of human red cells in liquid nitrogen with hydroxyethyl starch. *Cryobiology.* 12:110–118.
8. Weatherbee, L., E. D. Allen, H. H. Spencer, S. M. Lindenauer, and P. A. Permoad. 1975. The effects of plasma on hydroxyethyl starch-preserved red cells. *Cryobiology.* 12:119–122.
9. Knight, C. A., A. L. DeVries, and L. D. Oolman. 1984. Fish antifreeze protein and the freezing and recrystallization of ice. *Nature (Lond.).* 308:295–296.
10. Knight, C. A., and J. G. Duman. 1986. Inhibition of recrystallization of ice by insect thermal hysteresis proteins: a possible cryoprotective role. *Cryobiology.* 23:256–262.
11. Knight, C. A., J. Hallett, and A. L. DeVries. 1988. Solute effects on ice recrystallization: an assessment technique. *Cryobiology.* 25:55–60.
12. Carpenter, J. F., and T. N. Hansen. 1992. Antifreeze protein modulates cell survival during cryopreservation: mediation through influence on ice crystal growth. *Proc. Natl. Acad. Sci. USA.* 89:8953–8957.
13. Chang, Z. H., T. N. Hansen, and J. G. Baust. 1991. The effects of AFP on the devitrification of cryoprotectant systems. *Cryo Letts.* 11:215–226.
14. Takahashi, T., A. Hirsh, E. Erbe, and R. J. Williams. 1988. Mechanism of cryoprotection by extracellular polymeric solutes. *Biophys. J.* 54:509–518.
15. Chang, Z. H., and J. G. Baust. 1991. Physical ageing of glassy state: DSC study of vitrified glycerol systems. *Cryobiology.* 28:87–95.
16. Bronshteyn, V. L., and P. L. Steponkus. 1992. Theoretical and experimental studies of the "ante-melting" phenomenon in hydroxyethyl starch solutions. *Cryobiology.* 29:708. (Abstr.)
17. Hew, C. L., S. Joshi, and N. -C. Wang. 1984. Analysis of fish antifreeze polypeptide by reversed-phase high-performance liquid chromatography. *J. Chromatogr.* 296:213–219.
18. Chakrabartty, A., V. S. Ananthanarayanan, and C. L. Hew. 1989. Structure-function relationship in a winter flounder antifreeze polypeptide I: Stabilization of an α-helical antifreeze polypeptide by charged-group and hydrophobic interactions. *J. Biol. Chem.* 264:11307–11312.
19. Körber, CH., M. W. Scheiwe, P. Boutron, and G. Rau. 1982. The influence of hydroxyethyl starch on ice formation in aqueous solutions. *Cryobiology.* 19:478–492.
20. Jochem, M., and CH. Körber. 1987. Extended phase diagram for the ternary solutions H2O-NaCl-Glycerol and H2O-NaCl-Hydroxyethylstarch (HES) determined by DSC. *Cryobiology.* 24:513–536.
21. MacKenzie, A. P. 1977. Non-equilibrium freezing behavior of aqueous systems. *Philos. Trans. R. Soc. Lond. B Biol. Sci.* 278:167–189.
22. Luyet, B. J. 1965. Phase transitions encountered in the rapid freezing of aqueous solutions. *Ann. NY Acad. Sci.* 125:505–521.
23. Rasmussen, D., and B. Luyet. 1969. Complementary study of

some non-equilibrium phase transitions in frozen solutions of glycerol, ethylene glycol, glucose and sucrose. *Biodynamica.* 10:319–331.

24. MacFarlane, D. R. 1985. Anomalous glass transition in aqueous propylene glycol solutions. *Cryo Lett.* 6:313–318.
25. Berens, A. R., and I. M. Hodge. 1982. Effects of annealing and prior history on enthalpy relaxation in glassy polymers. I. Experimental study on poly (vinyl chloride). *Macromolecules.* 15:756–761.
26. MacFarlane, D. R., and M. Fargoulis. 1986. Theory of devitrification in multicomponent glass forming systems under diffusion control. *Phys. Chem. Glasses.* 27:228–234.
27. Forsyth, M., and D. R. MacFarlane. 1986. Recrystallization revisited. *Cryo Lett.* 7:367–378.
28. Petrie, S. B. 1972. Thermal behavior of annealed organic glasses. *J. Polym. Sci. Part A2* 10:1255–1272.
29. DeVries, A. L. 1986. Antifreeze glycopeptides and peptides: interactions with ice and water. *Methods Enzymol.* 127:293–303.
30. Knight, C. A., C. C. Cheng, and A. L. DeVries. 1991. Adsorption of α-helical antifreeze peptides on specific ice crystal surface planes. *Biophys. J.* 59:409–418.
31. Rapatz, G., and B. Luyet. 1968. Patterns of ice formation in aqueous solutions of polyvinylpyrrolidone and temperature of instability of frozen solutions. *Biodynamica.* 10:149–166.
32. Burgers, W. G. 1963. Principles of recrystallization. *In* The Art and Science of Growing Crystals. J. J. Gilman, editor. Wiley, New York. 416–450.
33. DeVries, A. L., and Y. Lin. 1977. Structure of a peptide antifreeze and mechanism of adsorption to ice. *Biochim. Biophys. Acta.* 495:388–392.
34. Yang, D. S. C., M. Sax, A. Chakrabartty, and C. L. Hew. 1988. Crystal structure of an antifreeze polypeptide and its mechanistic implications. *Nature (Lond.).* 333:232–237.
35. Raymond, J. A., P. Wilson, and A. L. DeVries. 1989. Inhibition of growth of nonbasal planes in ice by fish antifreezes. *Proc. Natl. Acad. Sci. USA.* 86:881–885.